Petroleum Science 21 (2024) 2677–2687

Contents lists available at ScienceDirect

Petroleum Science

journal homepage: www.keaipublishing.com/en/journals/petroleum-science

Original Paper

Natural rubber latex as a potential additive for water-based drilling fluids

Jun Yang [a, b], Guan-Cheng Jiang [a, b, *], Jing-Tian Yi [a, b], Yin-Bo He [a, b], Li-Li Yang [a, b], Teng-Fei Dong [a, b], Guo-Shuai Wang [c]

[a] College of Petroleum Engineering, China University of Petroleum (Beijing), Beijing 102249, China
[b] National Engineering Research Center of Oil & Gas Drilling and Completion Technology, Beijing 102249, China
[c] Changqing Drilling General Company, CNPC Chuanqing Drilling Engineering Company Limited, Xi'an 710021, Shaanxi, China

ARTICLE INFO

Article history:
Received 22 August 2023
Received in revised form
19 April 2024
Accepted 25 April 2024
Available online 26 April 2024

Edited by Jia-Jia Fei

Keywords:
Natural materials
Water-based drilling fluids
Natural rubber latex
Bentonite suspensions
Filtration loss

ABSTRACT

The environmental hazards and "carbon footprint" of oil and gas drilling can be significantly reduced by replacing traditional petroleum-based chemical additives with natural materials derived from plants and animals. This paper explored for the first time the interaction mechanism between natural rubber latex (NRL) and bentonite suspensions (BTs) through a series of characterization experiments, as well as the potential applications in water-based drilling fluids (WBDF). The gel viscoelasticity experiments showed that NRL could decrease the consistency coefficient (k) and flow index (n) of BTs, and enhance the shear thinning performance of BTs as pseudo-plastic fluids. In addition, 0.5 w/v% NRL not only increased the critical yield stress and strengthened the structural strength between the bentonite particles, but also facilitated the compatibility of pressure loss and flow efficiency. The evaluation of colloidal stability and WBDF performance indicated that NRL particles could promote the hydration and charge stability on the surface of BTs particles, and optimize the particle size distribution and flow resistance of WBDF under the "intercalation-exfoliation-encapsulation" synergistic interaction. Moreover, NRL can improve the rheological properties of WBDF at high temperatures (<150 °C), and form a dense blocking layer by bridging and sealing the pores and cracks of the filter cake, which ultimately reduces the permeability of the cake and the filtration loss of WBDF.

1. Introduction

As greenhouse gas emissions have a negative impact on the ecosystem, many countries with strict environmental regulations required that the use of petroleum-based chemical additives in oil and gas drilling be minimized or eliminated, and that natural materials with a lower "environmental footprint" be used as an alternative to meet the needs of oil and gas drilling (Razali et al., 2018; Moustakas et al., 2020). Drilling fluid (DF), the fluid medium that remains in close contact with the formation throughout the oil and gas drilling process, has always required the addition of various types and functions of chemical additives to clean the wellbore, transport cuttings, cool and lubricate the drilling bit and maintain formation stability (Aftab et al., 2017; Jiang et al., 2022), yet these petroleum-based chemical additives pose varying degrees of ecological threat to the surface and subsurface environments (air, soil and water) around the wellsite (Rana et al., 2019). Based on the dispersant, DF can be divided into water-based drilling fluids (WBDF), oil-based drilling fluids (OBDF) and gas drilling fluids, with WBDF being the preferred choice for field engineers and researchers due to their relative eco-friendliness (Li et al., 2022a; Yang et al., 2023). Traditional WBDF add bentonite to water to form a colloidal suspension to meet the initial drilling requirements, in addition to a variety of chemical additives to stabilize rheology, control filtration, inhibit clay expansion, hydration, and ultimately to ensure smooth drilling operations (Ahmed et al., 2019; Gamal et al., 2020).

At present, some natural materials have been studied and successfully applied in WBDF by many scholars, such as cellulose (Li et al., 2022b; Liu et al., 2022a), lignin (Sternberg et al., 2021) and

* Corresponding author. College of Petroleum Engineering, China University of Petroleum (Beijing), Beijing 102249, China.
E-mail address: 15600263100@163.com (G.-C. Jiang).

https://doi.org/10.1016/j.petsci.2024.04.012

starch (Le Corre et al., 2010; Ricky et al., 2022), which are the most widespread in nature. These materials have the ability of rheology improvement and filtration control in WBDF through artificial chemical modification (Ikram et al., 2021). In addition, some researchers have collected natural materials directly from the local environment and applied them as additives in a series of interesting applications, some statistics are shown in Table 1.

Natural rubber latex (NRL) is a natural material from a wide range of sources (it can be produced from more than 2000 plants), collected from the bark of trees in a milky white colloidal suspension (Gong et al., 2013; Wichaita et al., 2021). Its main component is cis-1,4-polyisoprene ($-C_5H_8-$) units, with a content of between 25% and 35%. The dispersion medium is water, with traces of proteins, carbohydrates, amino acids, fats, inorganic salts, etc. (Nawamawat et al., 2011; Rochette et al., 2013). Currently, major global NRL production areas are concentrated in many countries and regions, including Thailand, Malaysia, Indonesia, India, China, etc. (Ali Shah et al., 2013). It is also currently an important industrial raw material in the fields of elastomers, biological tissue repair, automobile tires and medical gloves due to its excellent physicochemical properties (Yin et al., 2019). Unlike conventional oil-based additives, it is extracted directly from tree bark without the need to modify it chemically, which is important in reducing the potential threat to the surrounding environment from chemical additives (Adibi et al., 2022). As far as we are aware, there is no published and cited research literature on the use of NRL in oil and gas drilling by research organizations or individuals.

Based on the above, this paper aims to investigate and evaluate NRL as a natural additive for WBDF and explore the value and potential of NRL application in WBDF. Firstly, we obtained the basic physical and chemical properties of NRL, such as molecular structure, heat, particle size and morphology based on conventional characterization, then explored the effects of NRL on the shear thinning behavior, rheological model and viscoelastic modulus of BTs, and finally evaluated the improvement of rheological properties and filtration capacity of WBDF. We also hope that this study will inspire more researchers to seek bio-alternatives to petroleum-based chemicals.

2. Material and methods

2.1. Materials

Natural rubber latex (NRL) is collected by Rubber Research Institute, Chinese Academy of Tropical Agricultural Sciences (Hainan Province, China). Bentonite (BT) was purchased from Weifang Huawei Bentonite Group Co. (Shandong Province, China), in accordance with the American Petroleum Institute (API) standards. Several commonly used chemical reagents including sodium bicarbonate ($NaHCO_3$), sodium hydroxide (NaOH) and potassium chloride (KCl) were purchased from Sinopharm Group Chemical Reagent Co. (Shanghai, China), Ltd in analytical purity. Several typical commercial WBDF additives including xanthan gum (XC), Polyanionic cellulose (PAC) and calcium carbonate ($CaCO_3$) are supplied by China Oilfield Services Limited Co. (Hebei Province, China). Non-fluorescent bitumen (NFA-25) and barite provided by China University of Petroleum (Beijing) Bo-Cheng Technology Co. (Beijing, China).

2.2. Characterization

The NRL samples were dispersed in deionized water (0.1 w/v%) and tested as follows: (1) the aqueous NRL solution was titrated onto a carbon film, and the dispersion state and microscopic morphology of NRL in the aqueous solution were then observed using TEM (Tecnai F20); (2) the particle size distribution of NRL particles was determined using Nano ZS particle size analyzer (Malvern Instruments Ltd., UK) to determine the particle size distribution of NRL particles. In addition, the observation and determination of NRL particles in BTs was performed using TEM and Nano ZS particle size analyzer.

The NRL samples were centrifuged, dried and prepared as thin films, and then the following tests were performed: (1) the main molecular structure and functional groups of NRL were determined by MagnaIR-560 spectrometer (Nicolet, USA) in the wavelength range of 4000~400 cm^{-1}; (2) the thermal properties of NRL were investigated using TG/DSC thermal analyzer (Netzsch, Germany) in a nitrogen environment to study the thermal properties of NRL in the temperature range of 25~600 °C, and the temperature was ramped up at 10 °C/min; (3) Gel Permeation Chromatography (GPC) was used to detect the molecular weight distribution of the main components of NRL, with THF as the mobile phase; (4) SEM (Hitachi SU8010) was used to observe the surface morphology of NRL films. In addition, SEM was used for the observation and determination of NRL in BTs and WBDF.

2.3. Preparation of BTs and WBDF

According to American Petroleum Institute (API) recommended standards (API RP 13B1–2019) and China Petroleum and Natural Gas Industries-Field Testing of Drilling Fluids-Part 1: Water-based Fluids (GB/T 16783.1–2014), the application potential and mechanism of NRL in WBDF were investigated.

Preparation of BTs: Dispersing 4 w/v% bentonite and 0.2 w/v% Na_2CO_3 in an aqueous solution at a shear rate of 10,000 rpm for 30 min, and then hydrating the bentonite suspensions (BTs) at

Table 1
Some statistics on the use of natural materials as additives in WBDF.

Materials	Application	Author(s)
Grass	Rheological modifier, filtration and pH control	Hossain et al. (2016), Al-Hameedi et al. (2019a)
Gum arabic	Rheological modifier	Ajayi et al. (2022)
Mandarin peels	pH reducer, viscosity modifier, fluid loss agent	Al-Hameedi et al. (2019b)
Notoginsenoside	Inhibitor of shale hydration	Sun et al. (2022)
Potato peels	A rheological modifier; filtration control agent	Al-Hameedi et al. (2019c)
Date seed	Fluid loss additive	Amanullah et al. (2016)
Okra mucilage	Clay swelling inhibitor	Murtaza et al. (2022)
Psyllium husk	Viscosity, filtration agent	Salmachi et al. (2016)
Corn starch	Rheology enhancer, Filtration reducer	Ricky et al. (2022)
Basil seed	Enhanced rheology, filtration, inhibition and lubrication	Gao et al. (2021)
Tea polyphenols	Fluid loss additive	Li et al. (2020a)
Gelatin	Shale hydration inhibitor	Li et al. (2018)

room temperature for 24 h, which was used as the base fluid for subsequent experiments.

Preparation of WBDF: To formulate a comprehensive water-based drilling fluid (WBDF), additives with different functions were sequentially added to the BTs under high-speed stirring conditions. In this paper, the composition and dosage of WBDF additives are shown in Table 2.

Hot roll aging procedure of WBDF: The drilling fluid was poured into a stainless-steel container and placed in a GW300-X high-temperature roller heating furnace (Qingdao, China), and heated and rolled at a certain temperature for 16 h.

2.4. Evaluation experiments of BTs

2.4.1. Rheological testing

A Haake MARS III rheometer (Thermo Scientific, Germany) was used to test separately the shear thinning, flow behavior and viscoelastic modulus of BTs with different NRL additions. The experimental temperature was maintained at 25 °C and a C35/1° conical plate rotor (35 mm diameter, 1.0° cone angle, 0.053 mm pitch) was used. Amplitude/frequency scanning viscoelastic modulus tests were performed for 12 to 0.1 Pa and 10 to 0.01 Hz frequency, and the linear viscoelastic range strain and frequency set for experiments were 1.0 Pa and 1.0 Hz, respectively. The viscosity and flow tests were carried out for shear rates in the range of 0.1–1000 s^{-1}, and rheological model fitting analysis were carried out using the HAAKE Rheology Win software. At present, Bingham, Power-Law, Carson and Herschel-Bulkley (H–B) are common rheological models in this field. Here, the classic Bingham model (Bingham, 1916) and the widely used H–B model (Herschel and Bulkley, 1926) equations have been compared:

$$\tau = \tau_0 + \mu_P \gamma \quad \left(\begin{matrix}\text{Bingham}\\ \text{Model}\end{matrix}\right) \tag{1}$$

$$\tau = \tau_0 + k\gamma^n \quad \left(\begin{matrix}\text{Herschel}-\text{Bulkly}\\ \text{Model}\end{matrix}\right) \tag{2}$$

where τ is the shear stress (Pa), τ_0 is the yield stress (Pa), μ_P is the plastic viscosity (mPa·s), γ is the shear rate (s^{-1}), k is the consistency coefficient (Pa·s^n), and n is the flow index.

2.4.2. Colloidal stability testing

Particle size distribution and zeta potential (ξ) are important evaluation indexes for the colloidal stability of bentonite particles (Liu et al., 2022b), and the effect of NRL on the colloidal stability of BTs was tested using a Nano ZS particle size analyzer (Malvern Instruments Ltd., UK). The BTs were diluted to 0.2 w/v% with deionized water, the pH of the solutions was adjusted using dilute hydrochloric acid (HCl) and sodium hydroxide (NaOH) solutions, and the PSD and ξ potentials were tested after the test temperature was set at 25 °C.

Table 2
Formulation of WBDF.

Component	Functions	Dosage
Water	Continuous phase	350 mL
Bentonite (BT)	Viscosity and filtration reducer	14 g
Sodium hydroxide (NaOH)	pH control agent	0.30 g
Xanthan gum (XC)	Improving viscosity	0.35 g
Polyanionic cellulose (PAC)	Controlling fluid loss	2.80 g
Non-fluorescent asphalt (NFA-25)	Plugging agent	10.5 g
Potassium chloride (KCl)	Shale inhibitor	24.5 g
Calcium carbonate ($CaCO_3$)	Reducing reservoir damage	17.5 g
Barite	Weighting agent	105 g

2.5. Evaluation experiments of WBDF

2.5.1. API rheological experiment

According to GB/T 16783.1–2014, the rheological parameters of WBDF were determined using a ZNN-D6 six-speed rotational viscometer (Qingdao Tongchun Instrument Co., China), and the readings of the indicator at different rotational speeds were recorded to calculate the rheological parameters, including apparent viscosity (*AV*), plastic viscosity (*PV*) and dynamic shear (*YP*), according to the following equations:

$$AV = \frac{\theta_{600}}{2}\ (\text{mPa}\cdot\text{s}) \tag{1}$$

$$PV = \theta_{600} - \theta_{300}\ (\text{mPa}\cdot\text{s}) \tag{2}$$

$$YP = \theta_{300} - PV\left(\frac{\text{lbf}}{100\text{ft}^2}\right) \tag{3}$$

where θ_{600}, θ_{300} are the respective 600 and 300 rpm readings. In addition, $Gel_{10\ s/10\ min}$ can be recorded directly from 3 rpm readings.

2.5.2. Filtration experiment under high temperature and high pressure

To simulate the actual filtration of drilling fluid under high-temp and high-pressure conditions in the deep reservoir. The heated WBDF is stirred at 10,000 rpm for 20 min and then poured into the GGS71-A High-temperature and High-pressure Filtration Loss Apparatus (Qingdao Tongchun Instrument Co., Ltd., China), which is sealed by adding drilling fluid standard filter paper and placed in a heated metal container. Connect the nitrogen gas and maintain a pressure difference of 3.5 MPa. The filtration loss of WBDF is equal to twice the volume of WBDF filtrate passing through the filter paper in 30 min. The above experimental steps are based on GB/T 16783.1–2014.

3. Results and discussion

3.1. Characterization of NRL

3.1.1. FTIR

As shown in Fig. 1(a), the characteristic peaks of the main functional groups are clearly observed. The peak at 841.54 cm^{-1} is attributed to the cis-1,4 structural unit of polyisoprene. The peak at 1444.43 cm^{-1} is a typical olefinic vibration peak due to the C=C stretching vibration, while the characteristic peaks at 2915.53 cm^{-1} are due to the C–H bond in the stretching vibration of the alkyl group in the alkyl group (Tanaka et al., 2009). The unsaturated cis-1,4-polyisoprene is the main component of NRL as shown by the comprehensive analysis (Buranov et al., 2010).

3.1.2. TGA

Fig. 1(b) shows the TGA curves of the NRL under a nitrogen atmosphere from 25 °C up to 600 °C. Above 100 °C, NRL began to exhibit slight mass loss due to loss of adsorbed and bound water not thoroughly dried in samples (Liu et al., 2023). The samples began to decompose systematically as the temperature increased to around 320 °C, and especially at 382 °C the sample decomposition rate reached its peak. Degradation was almost complete at 480 °C, and 98.28% of the total mass was lost throughout the process, which included not only simple thermal decomposition but also

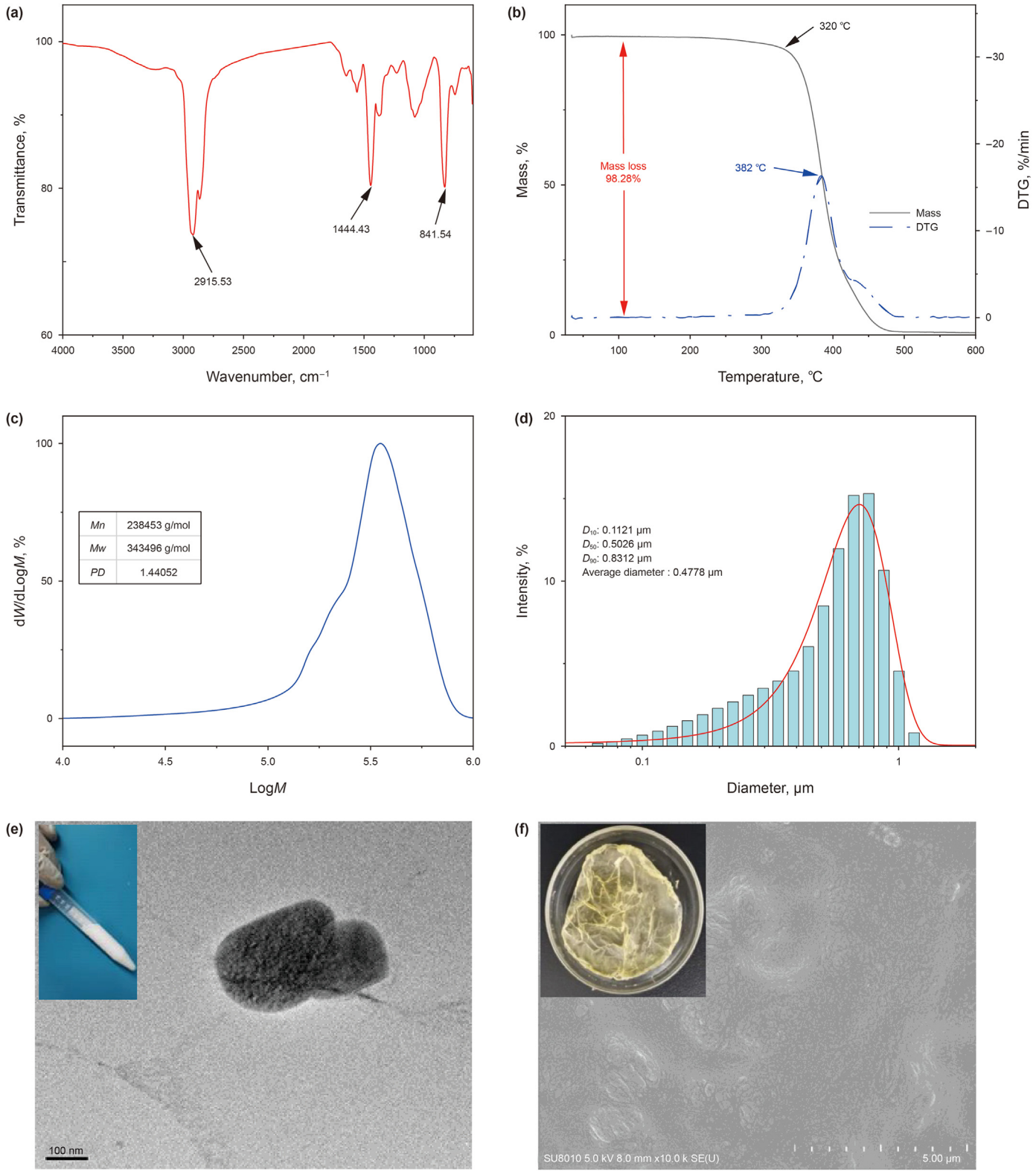

Fig. 1. Characterization results of NRL: (**a**) FTIR; (**b**) TGA; (**c**) GPC; (**d**) PSD; (**e**) Emulsion and TEM photographs; (**f**) Solid film and SEM photographs.

continuous breakage of polymer chains in the samples (Ma et al., 2023). As the NRL molecular chain contains unsaturated double bonds, the sample may also be accompanied by the addition reaction of double bonds to form polymers as the temperature rises, so the NRL has a high decomposition temperature (320 °C), which is conducive to the expansion of its application in high-temperature drilling fluids.

3.1.3. GPC

Fig. 1(c) shows the GPC curve of NRL, where the number average molecular weight (*Mn*), weight average molecular weight (*Mw*) and polydispersity index (*PD* = *Mw*/*Mn*) are 238,453 g/mol, 343,496 g/mol and 1.44052, respectively. And the individual peaks and *PD* values in the graph may indicate that the molecular weight distribution of the main component of the NRL molecular chain (cis 1,4-polyisoprene) is relatively uniform (Buranov et al., 2010).

3.1.4. PSD

Fig. 1(d) shows the aqueous solution of 0.1 w/v% NRL and its measured particle size distribution, with an overall maximum difference of one order of magnitude in the size distribution, which can be attributed to the small amount of protein and impurity particles present in the fresh latex product. The cumulative particle size distribution shows that the particle size distribution of NRL is concentrated between 0.1 and 1 μm, with a mean size of 0.4778 μm, the median particle size D_{50} = 0.5026 μm, and D_{10} and D_{90} of 0.1121 and 0.8312 μm, respectively.

3.1.5. TEM and SEM

In Fig. 1(e), the initial state of NRL (stable liquid emulsion) is shown as irregularly contoured oval particles under TEM, and the observed particle size is basically consistent with the test results in the PSD curve. The surface characteristics of NRL film were observed by SEM, as shown in Fig. 1(f). The surface of the NRL film is smooth, and there is a slightly raised structure in some areas, and some of the particles can be observed to be piled up and raised under magnification.

3.2. Performance improvement of NRL on BTs

3.2.1. Shear-thinning behavior

WBDF must have low viscosity at high shear rates (at the drilling bit) to help fracture the rock, and high viscosity at low shear rates (in the wellbore annulus) to help suspend the drill cuttings, so the shear thinning properties play an important role for WBDF to achieve suspension, carry the cuttings, clean the wellbore and ensure successful drilling of the formation (Wang et al., 2018). BTs is the basic dispersant of WBDF in the traditional sense and BTs is the primary dispersant of WBDF, Fig. 2 shows the variation curves of viscosity and shear stress with shear rate after different levels of NRL were added to BTs, the experimental procedure was carried out as described in 3.2.1. In Fig. 2(a), with the gradually increasing shear rate (0.1–1000 s^{-1}), all the suspensions showed a certain shear thinning behavior. While the BTs with 0.5 w/v%–2.0 w/v% NRL, showed a lower viscosity and a stronger shear thinning behavior in comparison (Singh et al., 2018). Additionally, the increase in NRL content contributed to the decrease in the shear stress of BTs from 12.17 to about 9.14 Pa (Fig. 2(b)), confirming that NRL improves shear thinning by reducing the apparent viscosity of BT suspensions.

The goodness-of-fit and related parameters of the BTs under the Bingham and Herschel Bulkley rheology models were comparatively investigated by collecting continuous datasets between 0.1 and 1000 s^{-1} for regression analyses. The results are shown in Table 3, R^2 (goodness of fit) indicates the degree of match between the actual measured curves and the rheological model, the minimum R^2 of the H–B model in the table is 0.9537, but it is still much larger than the maximum value of the R^2 (0.8266) under the Bingham model, this is due to the fact that the addition of the NRL as an emulsion reduces the yield stress after BTs, which contributes to the more pronounced pseudo-plastic fluid characteristics of the suspensions, and thus the H–B model as a typical pseudoplastic fluid model has a better fit than the plastic fluid (Bingham model) (Ouaer et al., 2018). Similar studies (Weir et al., 1996) have shown that both the H–B model and the Bingham model represent the flow properties of actual drilling fluids better in the medium and higher shear rate ranges. However, in the lower shear rate range, the H–B model is closer to the flow properties of actual drilling fluids (Saasen et al., 2020). Therefore, the Herschel Bulkley model can be used to predict the behavior of drilling fluids during flow, whereas the Bingham plasticity model can sometimes only predict trends (Wisniowski et al., 2020). In addition, in the statistics of the relevant parameters of the H–B Model, both the consistency coefficient (*k*) and the flow index (*n*) of BTs gradually decline with the increase of NRL content. The *k* value reflects the pumpability of the suspension to a certain extent, and lower *k* values are favorable to increase the drilling speed (Huang et al., 2016). The *n* value measures the ability of shear thinning property of non-Newtonian fluids, and the smaller the value of *n*, the more shear thinning property. The *k* and *n* values of BTs containing 2.0 w/v% NRL were 1.020 and 0.073, respectively, which were much lower than those of

Table 3
Fitted parameters for rheological models.

	Bingham Model			H–B Model			
	τ_0, Pa	μ_P, Pa·s	R^2	τ, Pa	k, Pa·s^n	n	R^2
BTs	4.508	0.0096	0.8266	1.973	1.672	0.257	0.9576
+0.5 w/v % NRL	4.012	0.0087	0.7778	1.835	1.438	0.171	0.9567
+1.0 w/v % NRL	3.816	0.0091	0.6757	1.363	1.387	0.077	0.9642
+1.5 w/v % NRL	3.696	0.0081	0.6371	1.346	1.369	0.071	0.9594
+2.0 w/v % NRL	3.482	0.0083	0.7421	1.342	1.020	0.073	0.9537

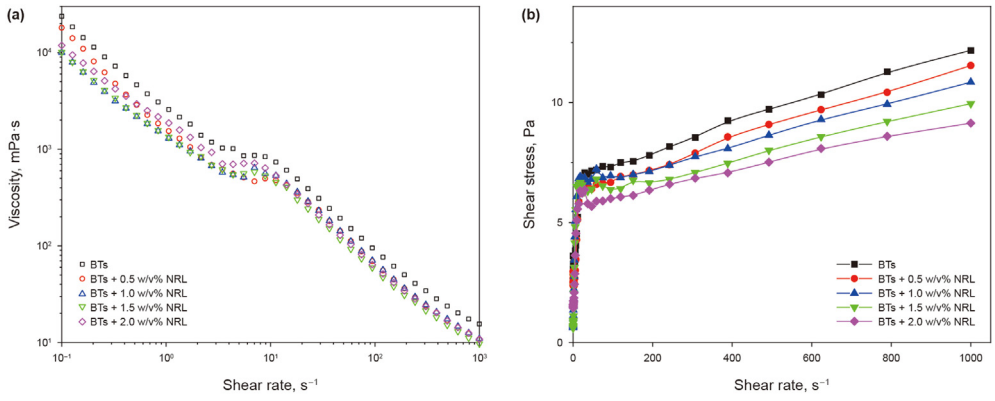

Fig. 2. Shear thinning of BTs containing (0~2.0 w/v%) NRL at different shear rates: (**a**) Change in viscosity; (**b**) Change in shear stress.

BTs of 1.672 and 0.257, which further confirmed the enhancement of the shear thinning property of NRL for the pseudoplastic fluid BTs.

3.2.2. Viscoelasticity modulus

The elastic modulus (G') and viscous modulus (G'') can reflect the structural strength of the internal gel network and the level of cyclic pressure loss of the colloidal suspension, and the WBDF maintains a higher gel strength to suspend drilling cuttings and solid phase materials, while a smaller cyclic pressure loss promotes mechanical efficiency (Abu-Jdayil et al., 2021). As shown in Fig. 3(a), when the shear stress is maintained constantly at 1.0 Pa, the BTs have a stable frequency dependence (typical gel characteristics) within the linear viscoelastic range (0.1–10 Hz), and the G' is always more than an order of magnitude higher than the G'', which proves that the BTs are elastically dominated by the flow behavior (Mathew et al., 2011), and the lower G'' only helps to reduce the circulating pressure loss to improve the drilling efficiency. When the frequency of 1.0 Hz is kept steady, the internal gel network structure of BTs under different shear stresses (0.1–12 Pa) changes as shown in Fig. 3(b). The stress value at the intersection of G' and G'' curves (the gel-sol transition point) in Fig. 3(b) is the critical shear stress of BTs, which represents the strength of the gel network structure of BTs. The critical shear stress of the initial BTs is about 6.85 Pa (black intersection), and the critical yield stress of BTs with 0.5 w/v% NRL is increased to 10.45 Pa (red intersection), so NRL is favorable to enhance the internal gel network strength and suspension of BTs (Wang et al., 2022).

In addition, the experiments have simulated the alteration of the network structure of WBDF during the drilling process. Fig. 4(a)–(e) show the states of BTs with NRL after 24 h of standing (drilling stopped), and it can be observed that BTs obviously flowed after the BTs suspensions were inverted (Fig. 4(a1)), while BTs with NRL (Fig. 4(b1)–(e1)) did not flow as a result of the formation of a solid gel structure network. The BT with NRL (Fig. 4(b1)–(e1)) are suspended at the bottom of the bottle without flowing due to the formation of a solid gel structure network, which is favorable for suspending the solid phase for a long-time during application. When slightly shaking (restarting), the BTs undergoes shear thinning based on the change of shear stress to resume the circulating flow (Fig. 4(a2)–(e2)), which is favorable for ensuring a lower operating start-up pressure and improving the efficiency of the drilling operation.

3.2.3. Colloidal stability

As shown in Fig. 5(a), the PSD showed a typical bimodal distribution (0.3 and 10 μm), but the peak of 10 μm in the suspension moved to the left (smaller particle size) after NRL addition. Comparing the ξ potentials of BTs at different pH (Fig. 5(b)) and NRL addition (Fig. 5(c)), the ξ potentials of BTs containing NRL in the same environment were lower, −33.4 mV at pH = 7, and −31.1 mV at 1.0 w/v%NRL, and the lower ξ potentials also indicated a stronger dispersion stability of BTs (Choo et al., 2015). As the pH increases leading to an increase in OH^- in solution, which leads to a change in the diffuse bilayer of bentonite particles and NRL particles, OH^- diluted the H^+ electrical properties causing a decrease in the overall potential of the BT, but the BT with the addition of NRL is always above the potential of the BT. Thus, the NRL dispersed the bentonite particles to some extent, confirmed that this phenomenon could clearly be attributed to the electrostatic interaction between the NRL and the bentonite particles. In other words, the NRL promoted the dispersion and exfoliation of the surface layer of the bentonite particles (Fig. 5(e)), enhanced the hydration and the stability of the bentonite particles. In addition, the PSD of NRL/BTs also formed a new particle size peak at 100 μm, which is obviously opposed to the above conclusion that "NRL promotes the dispersion of BTs particles", so what is the mechanism from which it originates? It has been shown that the montmorillonite in bentonite particles forms a structure similarly to a "house of cards" with face-to-face, side-to-side and side-to-side stacking behaviors (Fig. 5(d)), and through the static dispersion of BTs (Fig. 5(f)), it can be observed that NRL can be attached to the surface of bentonite to enclose BTs particles. Hence, NRL may have some flocculation or encapsulation effects in addition to the electrostatic effects (Stephen et al., 2006).

3.3. Rheology and filtration control properties of NRL in WBDF

3.3.1. Rheological enhancement

As shown in Fig. 6(a)–(d), the role of NRL was evaluated by testing the variation of rheological parameters of conventional natural polymer WBDF, including *AV*, *PV*, *YP*, and *Gel*, after aging 16 h at different temperatures (120, 140, and 150 °C). In general, the *AV*, *PV*, and *YP* of the conventional natural polymer WBDFs were basically stabilized at 140 °C and at temperatures lower than this temperature, where most of the natural polymer materials still have high molecular weights (Tanaka et al., 2009) to maintain the rheological properties of WBDF. At the same time, the experimental data showed that NRL significantly improved the viscosity and shear stress of WBDF, the *AV* increased from 44 to 49 mPa·s to about 60 mPa·s (Fig. 6(a)), the *PV* increased about 6 mPa·s (Fig. 6(b)), the *YP* increased 5–7 lbf/100 ft^2 (Fig. 6(c)), and the static shear stress was also slightly improved (Fig. 6(d)). When the temperature was increased from 140 to 150 °C, the all parameters of WBDF dropped dramatically, with a loss of about 30% or so in *AV*

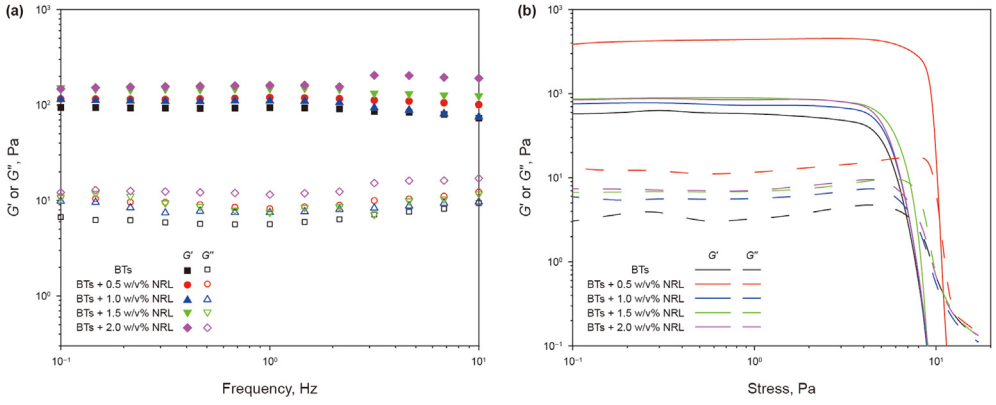

Fig. 3. The G' and G'' of BTs containing (0~2.0 w/v%) NRL under different test conditions: (**a**) Shear stress of 1.0 Pa; (**b**) Frequency of 1.0 Hz.

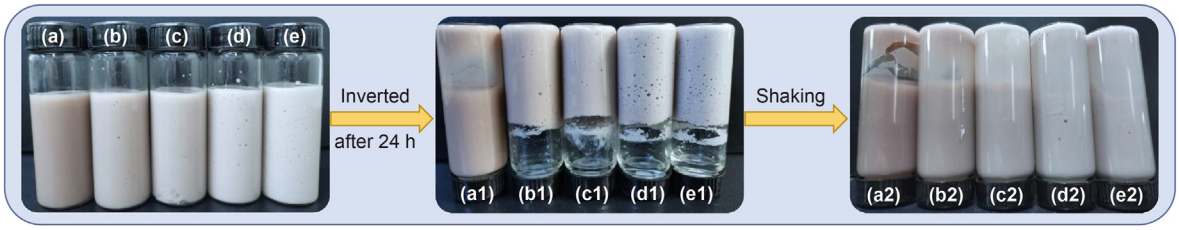

Fig. 4. The suspension status of BTs containing 0 w/v%, 0.5 w/v%, 1.0 w/v%, 1.5 w/v%, 2.0 w/v% NRL respectively: (**a**–**e**) Original status; (**a1**–**e1**) Inverted after 24 h; (**a2**–**e2**) After slight shaking.

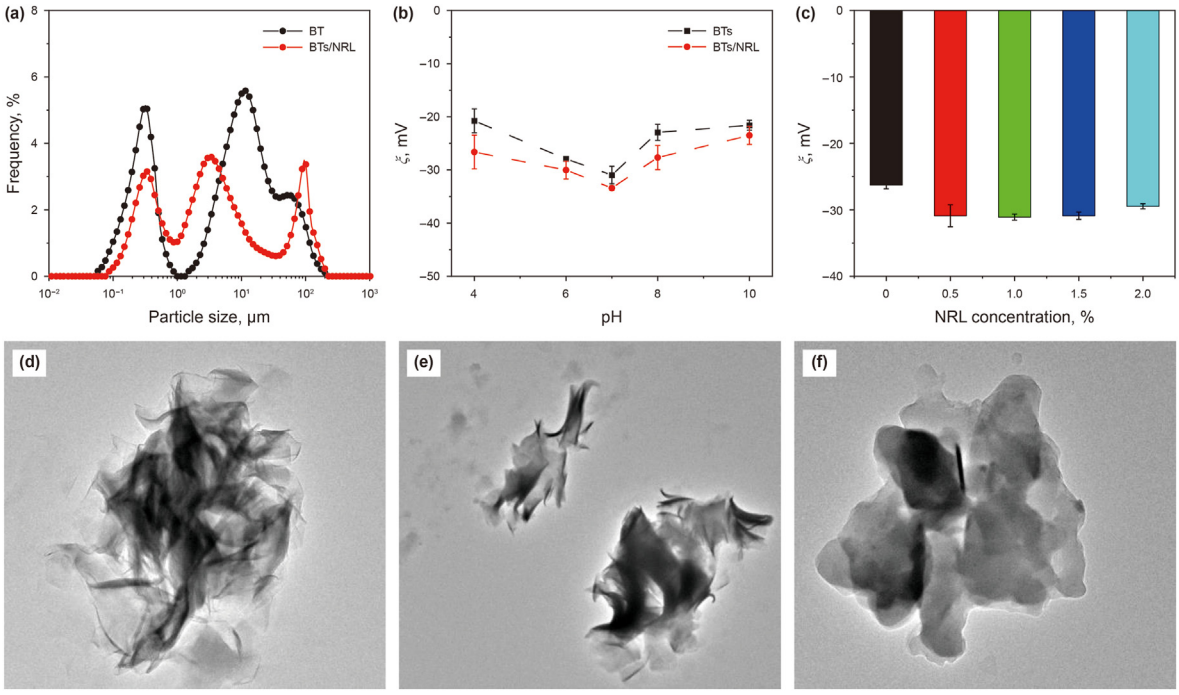

Fig. 5. Evaluation of the colloidal stability of BTs: (**a**) The PSD of BTs and BTs containing NRL; (**b**) The zeta of BTs and BTs containing NRL between pH 4 and 10; (**c**) The zeta of BTs containing 0 w/v%, 0.5 w/v%, 1.0 w/v%, 1.5 w/v%, 2.0 w/v% NRL respectively; (**d**) The original structure of BTs; (**e**) The exfoliated structure of BTs caused by NRL; (**f**) The BTs particles encapsulated by NRL.

(12–17 mPa·s), and a drop of more than 50% in *YP* and *Gel* (7–11 lbf/100 ft^2), and the decreasing trend of the rheological parameters of the WBDF with the addition of NRL was also obvious on this basis. This change is not only due to the rapid degradation of natural polymer additives at high temperatures, but also may originate from the thermal dehydration and gel disintegration of bentonite particles (Choo et al., 2015). Of course, the results of this experiment also proved that NRL can significantly improve the rheological parameters, rock carrying and wellbore cleaning efficiency of WBDF at formation temperatures lower than 150 °C.

3.3.2. Filtration control

The formation of a thin and dense filter cake on the well wall, which controls the penetration of filtration loss into the formation, enables WBDF to effectively slow down the occurrence of formation clay mineral hydration expansion and reservoir sensitivity damage, ensuring well stability and restoration of oil and gas production capacity at high temperatures (Yang et al., 2023). At 120 and 140 °C, the HTHP filtration loss of WBDF decreased by 3 and 4.5 mL, respectively. As the addition of NRL, the filtration loss control ability of WBDF was basically stable when the temperature was increased to 150 °C (Fig. 7(a)). The thickness of the filter cake can usually represent the tightness of the particle accumulation in the WBDF and the quality of the well wall (Siddig et al., 2022), and the permeability of the filter cake with high temperature destruction increases with the increase in thickness, which cannot effectively prevent the intrusion of solids and liquids from the well into the formation (Siddig et al., 2020). SEM observation of the filter cake (Fig. 7(b)) showed that the polymer and bentonite particles on the surface of the filter cake were degraded or dehydrated at high temperature, forming channels and micro-fractures of different levels (Fig. 8(a)–(c)), which provided a channel for further intrusion of drilling fluid. In contrast, at the same image size, a uniform film of NRL was observed on the solid phase particles of the filter cake, which partially blocked the microscopic pore spaces created by the high temperature, greatly improving the quality and reducing the permeability of the filter cake (Fig. 8(d)–(f)). Continuous enlarged views of the pore spaces of the filter cake clearly showed a large number of flakes and gel structures (Fig. 8(g)–(i)), which are rubber solids formed by the NRL during the high temperature water loss process, which could connect and fill the blockage and improve the gel strength of the filter cake, and reduce the high-temperature filtration loss of WBDF and the permeability of the filter cake effectively under a variety of functions.

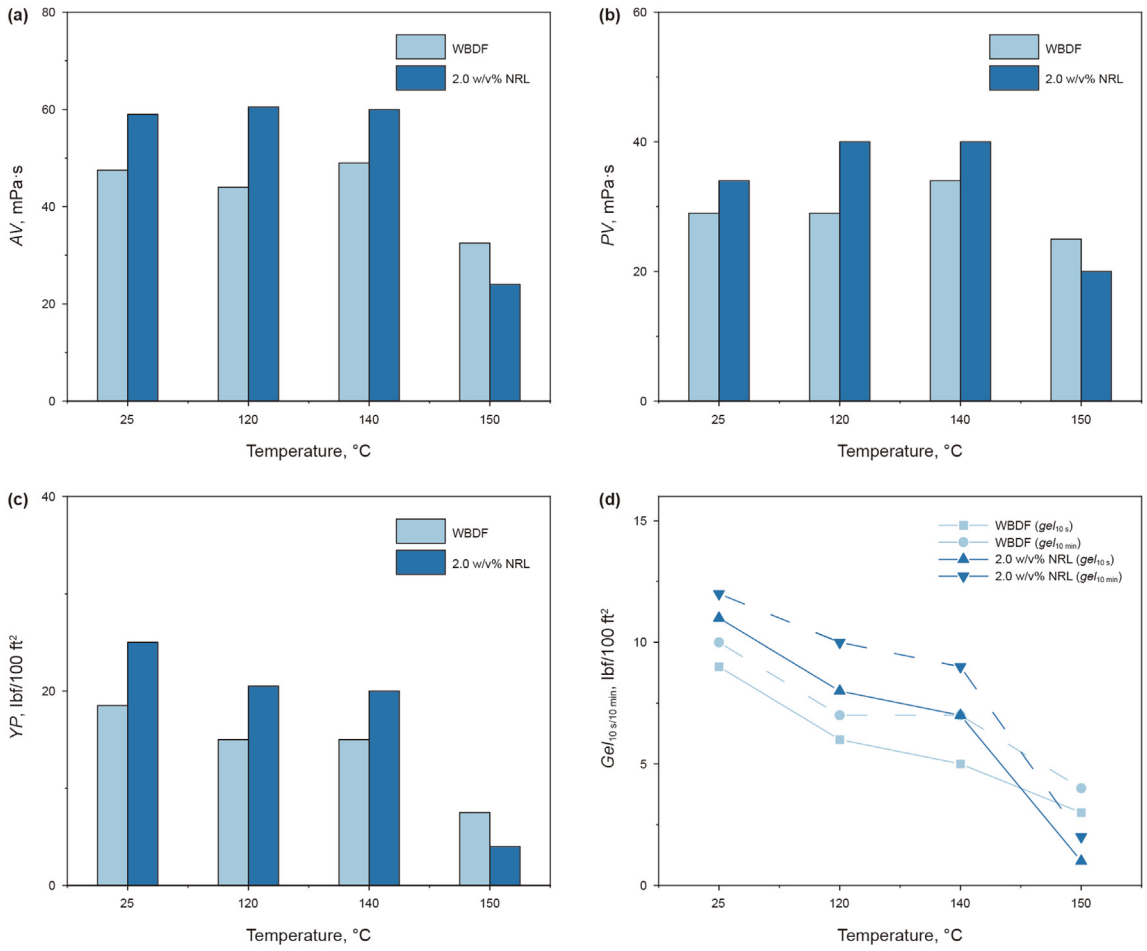

Fig. 6. Variation of rheological parameters of WBDF at different temperatures: (**a**) Apparent Viscosity; (**b**) Plastic Viscosity; (**c**) Yield press; (**d**) Gel Strength.

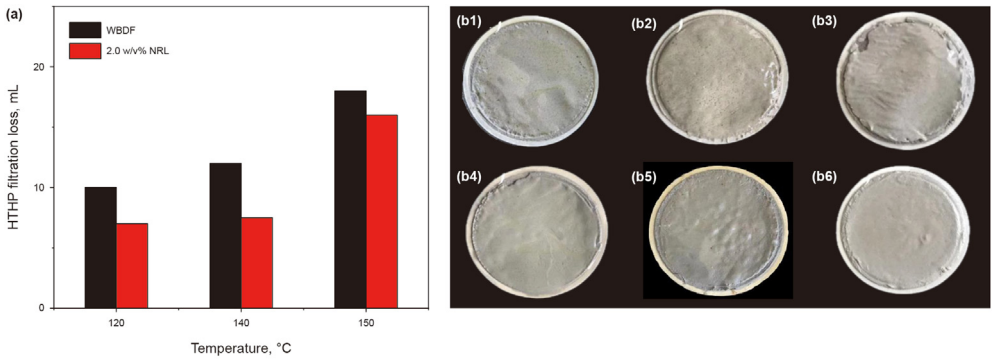

Fig. 7. The filter loss control performance of WBDF at 120, 140 and 150 °C: (**a**) The filter loss volume; (**b**) Filter cake shapes.

3.3.3. Potential mechanisms

Potential mechanisms of operation are analyzed in Fig. 9. Typically, the bentonite particles in BTs are hydrated, swollen and dispersed by water molecules, and at the same time the surface is negatively charged, in addition to forming a "card" structure with a certain spatial potential resistance, which is to some extent conducive to improving the rheology of drilling mud, promoting the formation of filter cake and reducing the intrusion of free water into the formation (Li et al., 2020b). This structure is somewhat conducive to improving the rheology of the drilling mud, promoting the formation of the filter cake and reducing the intrusion of free water into the formation. However, at high temperatures, the attachment of bentonite particles to water is weakened and dewatering of BTs leads to structural loosening and reduced electrostatic repulsion (Chatterjee et al., 2009), making it difficult to control rheology and drilling fluid loss. Fortunately, the surface of NRL particles has proteins (carboxyl groups) and phospholipids (phosphoryl groups) that can provide a negative charge (Wei et al., 2022), and under high-speed shear, NRL inserts into the clay interlayer and discharges some of the interlayer water molecules, and then disaggregates or peels off flocculated bentonite particles based on homogeneous charge repulsion to maintain the colloidal

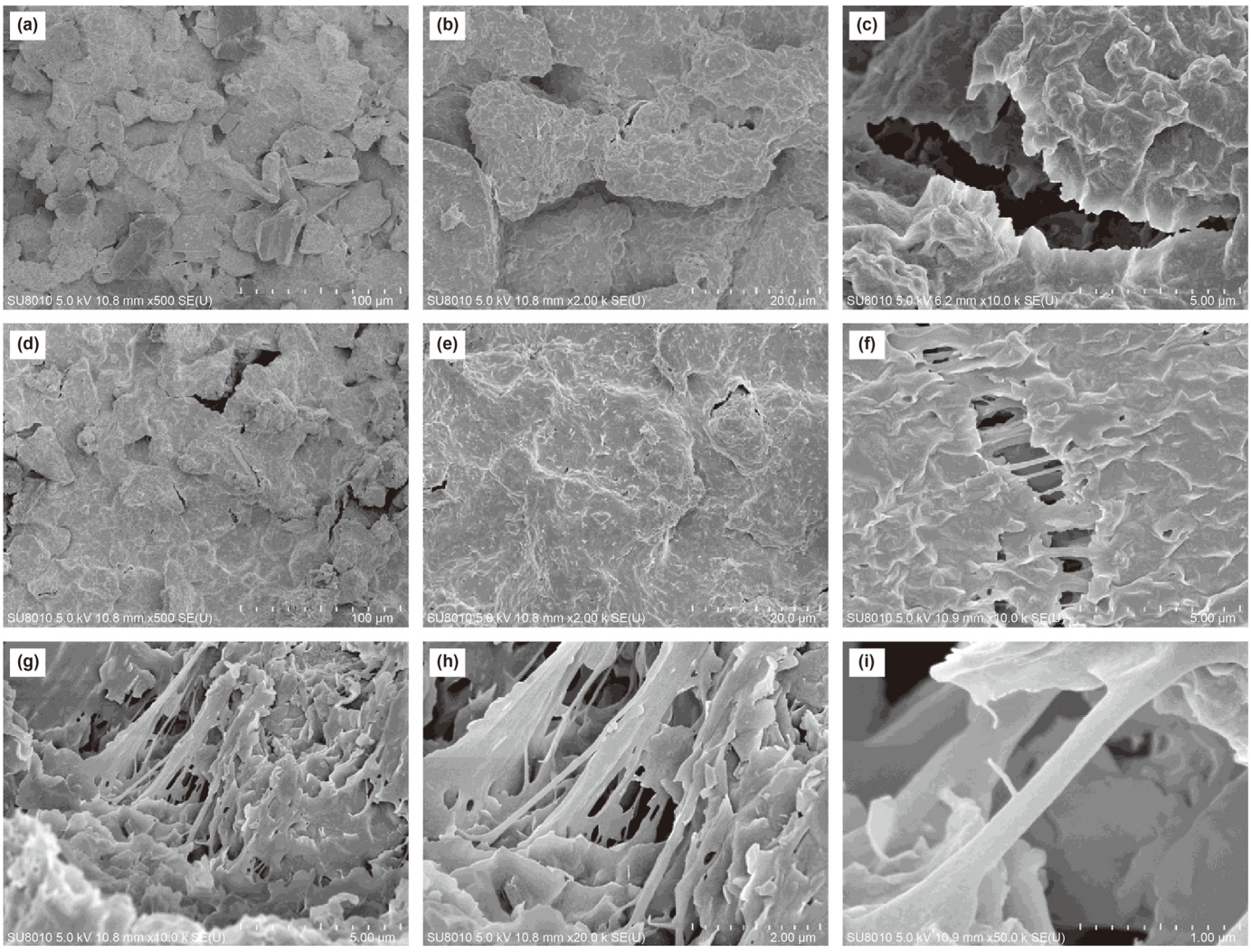

Fig. 8. The SEM of the microstructure of filter cake: (**a**–**c**) The WBDF at 100, 20 and 5 μm respectively; (**d**–**f**) The WBDF containing 2 w/v% NRL at 100, 20 and 5 μm respectively; (**g**–**i**) The WBDF containing 2 w/v% NRL at 5, 2 and 1 μm respectively.

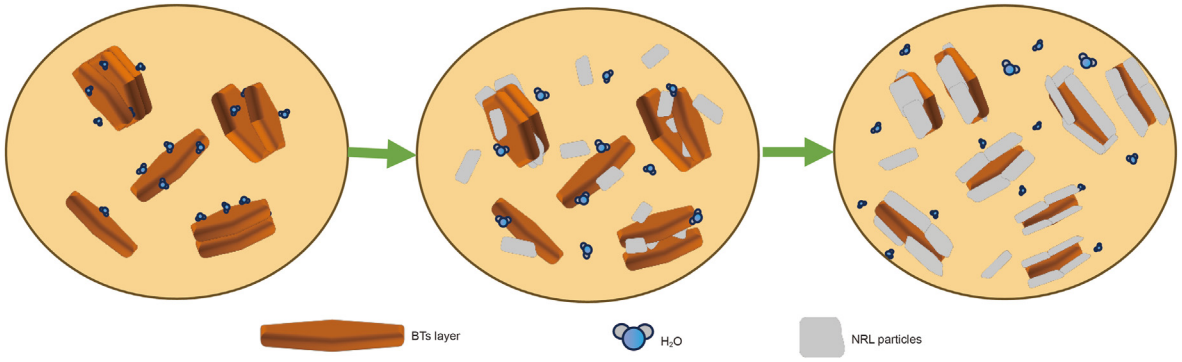

Fig. 9. Schematic illustration of the rheological and filtration control mechanisms of the NRL.

dispersion status at high temperatures. In addition, with the increasing amount of NRL and a large number of adsorption on the surface of bentonite particles, the unsaturated bonds and hydrogen bonds in the NRL at high temperatures to generate rubber polymer (Tanaka et al., 2009) covering bentonite particles, the accumulation of the coating tightly increases the interaction strength between the particles to maintain the rheological properties of the bentonite water-based fluid, the filling of the pores and microcracks of the BTs filter cake by the encapsulant helps to form a compact and dense blocking layer, which reduces filtration loss at high temperature and high pressure. As the temperature continues to rise (>140 °C), NRL, as a natural material, inevitably undergoes thermal degradation (Andler, 2020), and BTs "gel" due to rapid water loss and massive coagulation, which makes it difficult for NRL to adhere

stably to the inorganic matrix and ultimately leads to degradation of drilling mud performance at higher temperature.

4. Conclusions

This study confirmed that Natural rubber latex (NRL) can effectively improve the colloidal stability of BTs, as well as have potential applications in rheology and filtration control of WBDF. NRL is directly derived from rubber trees and has cis-1,4-polyisoprene as the main structural unit, in addition to unsaturated groups in the molecular chain. With the addition of NRL, the interaction between the solid and solid-liquid phases in the BTs was weakened, the *AV* of the suspensions was reduced, and the pseudoplastic rheological behavior (shear thinning property) of the BTs was enhanced under the H–B Model. By adding a small amount of NRL (0.5 w/v%), the critical shear stress of the BTs was increased to 10.45 Pa, which greatly improved the internal gel strength and suspension properties. In addition, NRL fills the pores and cracks of the drilling fluid filter cake under the joint interaction of "insertion-exfoliation-encapsulation", which improves the gel strength of the filter cake and forms a dense blocking layer, and effectively reduces the high-temperature and high-pressure filtration loss of WBDF, and the permeability of the filter cake. In future work, we hope to further develop the applicability of NRL at higher temperatures (>140 °C) through molecular modification or organic-inorganic composite research through polymerizable groups. Overall, this research could provide a "green alternative" in the search for environmentally friendly alternatives to petroleum-based chemical treatments for WBDF.

Conflict of interest

The authors declare no potential conflict of interest.

CRediT authorship contribution statement

Jun Yang: Writing – review & editing, Writing – original draft, Methodology, Investigation, Data curation, Conceptualization. **Guan-Cheng Jiang:** Writing – review & editing, Validation, Supervision, Resources, Project administration, Funding acquisition. **Jing-Tian Yi:** Writing – review & editing, Visualization, Investigation, Data curation, Conceptualization. **Yin-Bo He:** Supervision, Resources, Project administration, Funding acquisition. **Li-Li Yang:** Supervision, Resources, Project administration, Funding acquisition. **Teng-Fei Dong:** Supervision, Resources, Project administration, Funding acquisition. **Guo-Shuai Wang:** Writing – review & editing, Methodology, Conceptualization.

Declaration of competing interest

The authors declare that they have no known competing financial interests or personal relationships that could have appeared to influence the work reported in this paper.

Acknowledgments

This work was supported by the National Natural Science Foundation of China (Grant No. 51991361 and Grant No. 51874329).

References

Abu-Jdayil, B., Ghannam, M., Ahmed, K.A., et al., 2021. The effect of biopolymer chitosan on the rheology and stability of Na-bentonite drilling mud. Polymers 13 (19), 3361. https://doi.org/10.3390/polym13193361.

Adibi, A., Valdesueiro, D., Mok, J., et al., 2022. Sustainable barrier paper coating based on alpha-1,3 glucan and natural rubber latex. Carbohydr. Polym. 282, 119121. https://doi.org/10.1016/j.carbpol.2022.119121.

Aftab, A., Ismail, A.R., Ibupoto, Z.H., et al., 2017. Nanoparticles based drilling muds a solution to drill elevated temperature wells: a review. Renew. Sustain. Energy Rev. 76, 1301–1313. https://doi.org/10.1016/j.rser.2017.03.050.

Ahmed, H.M., Kamal, M.S., Al-Harthi, M., 2019. Polymeric and low molecular weight shale inhibitors: a review. Fuel 251, 187–217. https://doi.org/10.1016/j.fuel.2019.04.038.

Ajayi, F., Adewole, S., 2022. The performance of gum Arabic on water-based drilling mud at high temperatures. SPE Nigeria Annual Int. Conf. Exhibition, Lagos, Nigeria. https://doi.org/10.2118/211982-MS.

Al-Hameedi, A.T., Alkinani, H.H., Dunn-Norman, S., et al., 2019a. Proposing a new eco-friendly drilling fluid additive to enhance the filtration properties of water-based drilling fluid systems. In: SPE Gas & Oil Technology Showcase and Conference. UAE, Dubai. https://doi.org/10.2118/198651-MS.

Al-Hameedi, A.T., Alkinani, H.H., Dunn-Norman, S., et al., 2019b. Environmental friendly drilling fluid additives: can food waste products be used as thinners and fluid loss control agents for drilling fluid?. In: SPE Symposium: Asia Pacific Health, Safety, Security, Environment and Social Responsibility. Kuala Lumpur, Malaysia. https://doi.org/10.2118/195410-MS.

Al-Hameedi, A., Alkinani, H.H., Dunn-Norman, S., et al., 2019c. Insights into the application of new eco-friendly drilling fluid additive to improve the fluid properties in water-based drilling fluid systems. J. Pet. Sci. Eng. 183, 106424. https://doi.org/10.1016/j.petrol.2019.106424.

Ali Shah, A., Hasan, F., Shah, Z., et al., 2013. Biodegradation of natural and synthetic rubbers: a review. Int. Biodeterior. Biodegrad. 83, 145–157. https://doi.org/10.1016/j.ibiod.2013.05.004.

Amanullah, M., Ramasamy, J., Al-Arfaj, M.K., et al., 2016. Application of an indigenous eco-friendly raw material as fluid loss additive. J. Pet. Sci. Eng. 139, 191–197. https://doi.org/10.1016/j.petrol.2015.12.023.

Andler, R., 2020. Bacterial and enzymatic degradation of poly(cis-1,4-isoprene) rubber: novel biotechnological applications. Biotechnol. Adv. 44, 107606. https://doi.org/10.1016/j.biotechadv.2020.107606.

Bingham, E.C., 1916. An Investigation of the Laws of Plastic Flow. US Government Printing Office. https://doi.org/10.6028/bulletin.304.

Buranov, A.U., Elmuradov, B.J., 2010. Extraction and characterization of latex and natural rubber from rubber-bearing plants. J. Agric. Food Chem. 58, 734–743. https://doi.org/10.1021/jf903096z.

Chatterjee, T., Chatterjee, S., Woo, S.H., 2009. Enhanced coagulation of bentonite particles in water by a modified chitosan biopolymer. Chem. Eng. J. 148, 414–419. https://doi.org/10.1016/j.cej.2008.09.016.

Choo, K.Y., Bai, K., 2015. Effects of bentonite concentration and solution pH on the rheological properties and long-term stabilities of bentonite suspensions. Appl. Clay Sci. 108, 182–190. https://doi.org/10.1016/j.clay.2015.02.023.

Gamal, H., Elkatatny, S., Adebayo, A., et al., 2020. Effect of exposure time on the compressive strength and formation damage of sandstone while drilling horizontal wells. J. Pet. Sci. Eng. 195, 107590. https://doi.org/10.1016/j.petrol.2020.107590.

Gao, X., Zhong, H.Y., Zhang, X.B., et al., 2021. Application of sustainable basil seed as an eco-friendly multifunctional additive for water-based drilling fluids. Petrol. Sci. 18, 1163–1181. https://doi.org/10.1016/j.petsci.2021.05.005.

Gong, Y., Liu, G., Peng, W., et al., 2013. Immobilization of the proteins in the natural rubber with dialdehyde sodium alginate. Carbohydr. Polym. 98, 1360–1365. https://doi.org/10.1016/j.carbpol.2013.08.001.

Herschel, W.H., Bulkley, R., 1926. Konsistenzmessungen von Gummi-Benzollösungen. Kolloid Z. 39, 291–300. https://doi.org/10.1007/BF01432034.

Hossain, M.E., Wajheeuddin, M., 2016. The use of grass as an environmentally friendly additive in water-based drilling fluids. Petrol. Sci. 13, 292–303. https://doi.org/10.1007/s12182-016-0083-8.

Huang, W., Leong, Y., Chen, T., et al., 2016. Surface chemistry and rheological properties of API bentonite drilling fluid: pH effect, yield stress, zeta potential and ageing behaviour. J. Pet. Sci. Eng. 146, 561–569. https://doi.org/10.1016/j.petrol.2016.07.016.

Ikram, R., Jan, B.M., Sidek, A., et al., 2021. Utilization of eco-friendly waste generated nanomaterials in water-based drilling fluids; state of the art review. Materials 14 (15), 4171. https://doi.org/10.3390/ma14154171.

Jiang, G., Sun, J., He, Y., et al., 2022. Novel water-based drilling and completion fluid technology to improve wellbore quality during drilling and protect unconventional reservoirs. Engineering 18, 129–142. https://doi.org/10.1016/j.eng.2021.11.014.

Le Corre, D., Bras, J., Dufresne, A., 2010. Starch nanoparticles: a review. Biomacromolecules 11, 1139–1153. https://doi.org/10.1021/bm901428y.

Li, J., Qiu, Z., Zhong, H., et al., 2022a. Effects of water-based drilling fluid on properties of mud cake and wellbore stability. J. Pet. Sci. Eng. 208, 109704. https://doi.org/10.1016/j.petrol.2021.109704.

Li, X.L., Jiang, G.C., Shen, X.L., et al., 2020a. Application of tea polyphenols as a biodegradable fluid loss additive and study of the filtration mechanism. ACS Omega 5, 3453–3461. https://doi.org/10.1021/acsomega.9b03712.

Li, X.L., Jiang, G.C., Shen, X.L., et al., 2020b. Poly-L-arginine as a high-performance and biodegradable shale inhibitor in water-based drilling fluids for stabilizing wellbore. Acs Sustain. Chem. Eng. 8, 1899–1907. https://doi.org/10.1021/acssuschemeng.9b06220.

Li, X.L., Jiang, G.C., Yang, L.L., et al., 2018. Study of gelatin as biodegradable shale hydration inhibitor. Colloid Surf. A-Physicochem. Eng. Asp. 539, 192–200. https://doi.org/10.1016/j.colsurfa.2017.12.020.

Li, X.L., Wang, K., Xian, L.Y., et al., 2022b. Carboxylated cellulose nanocrystals as

environmental-friendly and multi-functional additives for bentonite water-based drilling fluids under high-temperature conditions. Cellulose 29, 6659–6675. https://doi.org/10.1007/s10570-022-04676-6.
Liu, J., Zhang, T., Sun, Y., et al., 2022a. Insights into the high temperature-induced failure mechanism of bentonite in drilling fluid. Chem. Eng. J. 445, 136680. https://doi.org/10.1016/j.cej.2022.136680.
Liu, K., Du, H.S., Liu, W., et al., 2022b. Cellulose nanomaterials for oil exploration applications. Polym. Rev. 62, 585–625. https://doi.org/10.1080/15583724.2021.2007121.
Liu, S., Zhang, C., Du, J.X., et al., 2023. Effect of dispersants on the stability of calcite in non-polar solutions. Colloid Surf. A-Physicochem. Eng. Asp. 672, 131730. https://doi.org/10.1016/j.colsurfa.2023.131730.
Ma, G., Zuo, H., Pang, S., et al., 2023. Anchoring polyamide active layer to improve the thermal stability of polyacrylonitrile composite forward osmosis membrane through interfacial enthalpic effect. Sep. Purif. Technol. 318, 123954. https://doi.org/10.1016/j.seppur.2023.123954.
Mathew, S., Varghese, S., George, K.E., et al., 2011. Rheological behaviour of layered silicate-natural rubber latex nanocomposites. Prog. Rubber Plast. Recycl. Technol. 27, 177–192. https://doi.org/10.1177/147776061102700304.
Moustakas, K., Loizidou, M., Rehan, M., et al., 2020. A review of recent developments in renewable and sustainable energy systems: key challenges and future perspective. Renew. Sustain. Energy Rev. 119, 109418. https://doi.org/10.1016/j.rser.2019.109418.
Murtaza, M., Ahmad, H.M., Zhou, X., et al., 2022. Okra mucilage as environment friendly and non-toxic shale swelling inhibitor in water based drilling fluids. Fuel 320, 123868. https://doi.org/10.1016/j.fuel.2022.123868.
Nawamawat, K., Sakdapipanich, J.T., Ho, C.C., et al., 2011. Surface nanostructure of Hevea brasiliensis natural rubber latex particles. Colloids Surf., A 390, 157–166. https://doi.org/10.1016/j.colsurfa.2011.09.021.
Ouaer, H., Gareche, M., Rooki, R., 2018. Rheological studies and optimization of Herschel-Bulkley parameters of an environmentally friendly drilling fluid using genetic algorithm. Rheol. Acta 57, 693–704. https://doi.org/10.1007/s00397-018-1110-z.
Rana, A., Arfaj, M.K., Saleh, T.A., 2019. Advanced developments in shale inhibitors for oil production with low environmental footprints – a review. Fuel 247, 237–249. https://doi.org/10.1016/j.fuel.2019.03.006.
Razali, S.Z., Yunus, R., Rashid, S.A., et al., 2018. Review of biodegradable synthetic-based drilling fluid: progression, performance and future prospect. Renew. Sustain. Energy Rev. 90, 171–186. https://doi.org/10.1016/j.rser.2018.03.014.
Ricky, E., Mpelwa, M., Wang, C., et al., 2022. Modified corn starch as an environmentally friendly rheology enhancer and fluid loss reducer for water-based drilling mud. SPE J. 27, 1064–1080. https://doi.org/10.2118/209195-PA.
Rochette, C.N., Crassous, J.J., Drechsler, M., et al., 2013. Shell structure of natural rubber particles: evidence of chemical stratification by electrokinetics and Cryo-TEM. Langmuir 29, 14655–14665. https://doi.org/10.1021/la4036858.
Salmachi, A., Talemi, P., Tooski, Z.Y., 2016. Psyllium husk in water-based drilling fluids: an environmentally friendly viscosity and filtration agent. In: The Abu Dhabi International Petroleum Exhibition & Conference. UAE, Abu Dhabi. https://doi.org/10.2118/183308-MS.
Siddig, O., Mahmoud, A.A., Elkatatny, S., 2020. A review of different approaches for water-based drilling fluid filter cake removal. J. Pet. Sci. Eng. 192, 107346. https://doi.org/10.1016/j.petrol.2020.107346.
Siddig, O., Mahmoud, A.A., Elkatatny, S., 2022. A review of the various treatments of oil-based drilling fluids filter cakes. J. Pet. Explor. Prod. Technol. 12, 365–381. https://doi.org/10.1007/s13202-021-01427-4.
Singh, M., 2018. The colloidal properties of commercial natural rubber latex concentrates. J. Rubber Res. 21, 119–134. https://doi.org/10.1007/BF03449165.
Stephen, R., Alex, R., Cherian, T., et al., 2006. Rheological behavior of nanocomposites of natural rubber and carboxylated styrene butadiene rubber latices and their blends. J. Appl. Polym. Sci. 101, 2355–2362. https://doi.org/10.1002/app.23852.
Sun, J.S., Wang, Z.L., Liu, J.P., et al., 2022. Notoginsenoside as an environmentally friendly shale inhibitor in water-based drilling fluid. Petrol. Sci. 19, 608–618. https://doi.org/10.1016/j.petsci.2021.11.017.
Saasen, A., Ytrehus, J.D., 2020. Viscosity models for drilling Fluids-Herschel-Bulkley parameters and their Use. Energies 13 (20), 5271. https://doi.org/10.3390/en13205271.
Sternberg, J., Sequerth, O., Pilla, S., 2021. Green chemistry design in polymers derived from lignin: review and perspective. Prog. Polym. Sci. 113, 101344. https://doi.org/10.1016/j.progpolymsci.2020.101344.
Tanaka, Y., Tarachiwin, L., 2009. Recent advances in structural characterization of natural rubber. Rubber Chem. Technol. 82, 283–314. https://doi.org/10.5254/1.3548250.
Wang, G.S., Jiang, G.C., Fu, Y., et al., 2022. pH-responsive water-in-oil emulsions with reversible phase inversion behavior stabilized by a novel dynamic covalent surfactant. J. Mol. Liq. 364, 120004. https://doi.org/10.1016/j.molliq.2022.120004.
Wang, K., Jiang, G.C., Liu, F., et al., 2018. Magnesium aluminum silicate nanoparticles as a high-performance rheological modifier in water-based drilling fluids. Appl. Clay Sci. 161, 427–435. https://doi.org/10.1016/j.clay.2018.05.012.
Wei, Y.C., Zhu, D., Xie, W.Y., et al., 2022. In-situ observation of spatial organization of natural rubber latex particles and exploring the relationship between particle size and mechanical properties of natural rubber. Ind. Crop. Prod. 180, 114737. https://doi.org/10.1016/j.indcrop.2022.114737.
Weir, I.S., Bailey, W.J., 1996. A statistical study of rheological models for drilling fluids. SPE J. 1, 473–486. https://doi.org/10.2118/36359-PA.
Wichaita, W., Promlok, D., Sudjaipraparat, N., et al., 2021. A concise review on design and control of structured natural rubber latex particles as engineering nanocomposites. Eur. Polym. J. 159, 110740. https://doi.org/10.1016/j.eurpolymj.2021.110740.
Wisniowski, R., Skrzypaszek, K., Malachowski, T., 2020. Selection of a suitable rheological model for drilling fluid using applied numerical methods. Energies 13 (12), 3192. https://doi.org/10.3390/en13123192.
Yang, J., Jiang, G., Wang, G., et al., 2023. Performance evaluation of polymer nanolatex particles as fluid loss control additive in water-based drilling fluids. Geoenergy Science and Engineering 223, 211462. https://doi.org/10.1016/j.geoen.2023.211462.
Yin, J., Hou, J., Huang, S., et al., 2019. Effect of surface chemistry on the dispersion and pH-responsiveness of chitin nanofibers/natural rubber latex nanocomposites. Carbohydr. Polym. 207, 555–562. https://doi.org/10.1016/j.carbpol.2018.12.025.